International Journal of Mechanical and Electrical Engineering
ISSN: 3005-9615 (Print), ISSN: 3005-7132 (Online) | Volume 4, Number 3, Year 2024
DOI: https://doi.org/10.62051/ijmee.v4n3.04
Journal homepage: https://wepub.org/index.php/IJMEE/index

Simulation and Analysis of Water-cooled Heat Dissipation of Industrial Silicon Burner based on ANSYS

Panpan Sun [1, a], Guangzhong Hu [1, 2, *], Ping Wang [1, 2], Lei Yang [1], Minhong Luo [3], Jinghao Yu [1]

[1] School of Mechanical Engineering, Sichuan University of Science & Engineering, Yibin 644000, China
[2] Key Laboratory of Process Equipment and Control Engineering in Sichuan Province Universities, Yibin 644000, China
[3] Sichuan Youseth Intelligent Technology Co., Ltd, Chengdu 610000, China
* Corresponding author: Guangzhong Hu (Email: hgzdhx@163.com), [a] 2730924562@qq.com

ABSTRACT

The performance of the water cooling system of a new type of burner plays an important role in the safe and stable operation of the whole equipment. The material properties of steel, such as yield strength and modulus of elasticity, deteriorate under high-temperature conditions, leading to a decrease in the structural load-bearing capacity, which will bring about potential safety hazards when the burner is in operation. In this paper, the coupled thermal-electrical model and fluid temperature field model of graphite electrode and electrode holder of the burner are established, and the water-cooled heat dissipation simulation of the electrode holder of the burner is carried out by taking into account the effects of radiant heat dissipation, air convection, electric current and fluid flow on the temperature of the burner when it is in operation. The simulation results show that: After the inlet flow rate of 42.54L/min liquid water cooling, the temperature of the collet is reduced to the safe temperature, and the wedge-shaped clamping block is below the maximum continuous working temperature of the material, and the temperature continues to decrease with the increase of inlet flow rate. In summary, the minimum inlet flow rate of the water cooling system for the burn-through device is 42.54 L/min.

KEYWORDS

Burn-in Apparatus; Electrode Holder; Thermo-electrical Coupling; Temperature Distribution; Water-Cooled Heat Dissipation.

1. INTRODUCTION

Silicon, as a fundamental raw material, has been widely used in various industrial fields such as chemical engineering, metallurgy, electronics, machinery manufacturing, aerospace, shipbuilding, and energy development[1]. As a high-energy product, industrial silicon has been the largest producer and consumer in the world since 1980 [2]. During the smelting process of industrial silicon, the core component of the furnace discharging robot—the burn-through device—relies on graphite electrodes to melt the furnace eye. Traditional burn-through devices in China are generally handheld. During operation, workers grip the handle to bring the front end of the burn-through device close to the furnace eye, where the graphite electrode generates an arc that uses the high temperature of the arc to melt the furnace eye. However, due to the high-temperature, high-current, and high-dust environment

in the furnace discharging area, there are significant safety risks for workers exposed to these conditions for extended periods [3,4]. During the discharging process under high-temperature environments and complex operating conditions, the burn-through device not only needs to withstand the high temperatures from the arc and furnace eye but also the heat generated by the graphite electrode due to the high current, causing the temperature of the burn-through device to exceed 1000°C.

During operation, if the temperature becomes too high, it can pose a risk to the normal use of the equipment. Therefore, water cooling is commonly used to dissipate heat from the device. Xie Yan et al.[5]designed a water cooling device for packaging machines to address the issue of excessive heat generated during the transmission process and the heating of the electrical control system components, cooling key parts such as the forming mold, blowing mold, and top plate. Xu Yufeng et al.[6]designed a cooling device for the punch of a forging machine to solve the problems of temperature rise and rigidity loss caused by long-term operation. The device can cool the punch through mist spraying or immersion. Zhang Bin et al.[7]addressed the issue of excessive heat generation in oil-immersed transformers, which can shorten the lifespan of the transformer or even cause accidents. Based on the temperature and flow simulation of a single heat sink, they proposed two water cooling devices and analyzed the temperature distribution of the transformer's finned heat dissipation system. Yue Xiaoyun[8] focused on the main components in an electric motor controller and employed a water cooling plate to ensure that the temperature did not exceed the thermal limit, performing thermal simulation analysis using ANSYS. Duan Huiqiang et al. [9] studied a single IGBT module in the traction inverter of a maglev train and designed a novel heat transfer embedded IGBT water cooling module. They also researched the impact of different fin designs and inlet flow rates on module performance. The new water cooling system reduced the module's maximum temperature by about 7.4%. Chen et al. [10] designed a new dual-channel water cooling structure that achieved internal circulation cooling without additional auxiliary devices. The results showed that low flow rates had a significant effect on the cooling efficiency, and the optimal cooling performance was achieved at a flow rate of 6 L/min. Liu Xiaoping et al. [11] invented a handheld burn-through device with a cooling chamber. Cooling water enters the chamber through an inlet pipe to cool the burn-through device, significantly lowering the overall temperature. Wu Junping et al. [12] proposed an industrial silicon burn-through device that replaces the graphite sleeve for electrode clamping with a circulating water pipe to cool the electrode below the conductor steel pipe. Hu Haifu et al. [13] developed a high-temperature smelting water-cooled burn-through device that employs a water-cooled structure to lower the temperature of the burn-through device, thereby extending its service life. Chang Jing et al. [14] proposed a furnace mouth burn-through device used in ferrosilicon production, utilizing a water-cooled mechanism on both sides of the electrode holder's fixed seat to address the issue of high-temperature damage to the clamping fixture.

In summary, scholars have conducted research on the water cooling heat dissipation of equipment, proposing various water cooling structures for burn-through devices, which provide important references for this study. However, in the metallurgical field, studies on the temperature field distribution of burn-through devices after heat dissipation are rarely addressed. This research focuses on a novel discharging device, considering the effects of the arc zone temperature, radiation heat dissipation, short circuit current, and the inlet flow rate of the water cooling fluid on the temperature during the operation of the burn-through device. The study investigates the temperature distribution of the electrode holder in the burn-through device under different currents and inlet flow rates. Based on the material's working temperature and simulation temperature, the safety of the burn-through device during operation is analyzed, providing a reference for the minimum inlet flow rate of the water cooling heat dissipation system to ensure the safe and stable operation of the burn-through device.

2. SIMULATION ANALYSIS MODEL AND METHOD

2.1. Burn-through Device Physical Model

The electrode holder of the burn-through device consists of four wedge-shaped clamping blocks, a chuck, a water-cooled sleeve, a butterfly oil cylinder, conductive copper pads, and other components. The electrode holder is fixed onto the cross arm of the burn-through device and is driven by the butterfly oil cylinder to move the wedge-shaped clamping blocks back and forth, controlling the clamping and releasing of the graphite electrode. The wedge-shaped clamping blocks and the chuck do not have conductive properties, so conductive copper pads are used to supply current to the graphite electrode.When the working current flows through the graphite electrode, it rapidly heats up to over 1000°C in a short time, transferring heat to the wedge-shaped clamping blocks and the chuck of the burn-through device. The center of the chuck must be water-cooled to ensure that the electrode holder maintains sufficient strength, reduces expansion, minimizes oxidation, and lowers resistance. The electrode sintering area is the weakest part of the entire electrode, and the electrode holder must provide adequate clamping force on the electrode [15]. If no cooling treatment is applied to the center of the chuck, excessive temperature could result in the electrode holder losing sufficient strength, which would negatively affect the discharge operation.

The materials used for the wedge-shaped clamping blocks and the chuck are S31008 stainless steel, while the inlet and outlet pipes and the water-cooled sleeve are made of 316L stainless steel. S31008 stainless steel begins to soften at temperatures exceeding 800°C, and many of its mechanical properties, such as stress resistance, start to continuously degrade. However, it can be used continuously at temperatures up to 1150°C.

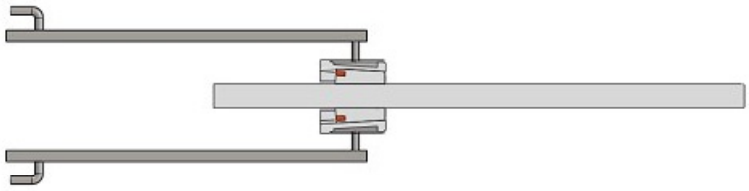

Fig 1. Cross-sectional Diagram of the Burn-through Device Physical Model

2.2. Burn-through Device System Coupling Model

Based on the simplified physical model above, before performing the analysis using software, the flow state of the fluid in the flow channels is determined by the Reynolds number (Re) [17]. The calculation formula for the Reynolds number is as follows:

$$Re = \frac{\rho u d}{\eta}$$

In the formula: ρ is the fluid density in kg/m³; u is the inlet flow velocity of the fluid in m/s; d is the inlet diameter of the fluid in meters; η is the dynamic viscosity of the fluid in kg/(m·s). The fluid used in this study is liquid water, with a density of 998.2 kg/m³. The inlet flow velocity is set to 0.5 m/s, and the inlet diameter of the fluid is 32.4 mm. The dynamic viscosity of water is 0.001003 kg/(m·s). Using formula, Re = 16122.47. According to the numerical range, when Re > 10000.0, the flow state of the fluid is in the turbulent flow region. Therefore, the fluid flow state is set to turbulent flow.

The primary heat source in the model is the Joule heat generated by the graphite electrode. According to Joule's law, the expression for Joule heat is:

$$Q_1 = I^2RT$$

In the formula: Q1 is the heat generated by the current, in joules (J); I is the current passing through the graphite electrode, in amperes (A); R is the resistance of the graphite electrode, in ohms (Ω); t is the time the current passes through the graphite electrode, in seconds (s).

The heat transfer during the burn-through device's cooling process occurs in three modes: conduction, convection, and radiation.

Heat conduction: According to Fourier's law and the law of energy conservation, the expression for heat conduction is [18]:

$$\rho c \frac{\partial T}{\partial t} = \lambda \left(\frac{\partial^2 T}{\partial x^2} + \frac{\partial^2 T}{\partial y^2} + \frac{\partial^2 T}{\partial z^2} \right) + qv$$

In the formula: ρ is the density of the object, in kg/m³; c is the specific heat capacity of the object, in J/(kg·℃);T is the temperature of the object, in ℃;t is time, in seconds (s);λ is the thermal conductivity of the object; qv is the heat source intensity within the graphite electrode, in W/m³.

Convective heat transfer: The convective heat transfer is simply described using Newton's cooling law [19], and the expression is:

$$\varphi = hA\Delta t$$

In the formula: φ is the convective heat transfer power, in watts (W); h is the convective heat transfer coefficient, in W/(m²·℃); A is the heat transfer area, in m²;Δt is the temperature difference between the clamping head or wedge block and the air, in ℃.

Radiative heat transfer: The expression for the radiative heat transfer power is:

$$q = \varepsilon \sigma S_d (T_1^4 - T_2^4)$$

In the formula: q is the radiative heat transfer power, in watts (W); ε is the emissivity; σ is the Stefan-Boltzmann constant, in W/(m²·K⁴); T1 and T2 are the temperatures of the graphite electrode and the wedge block surface, in Kelvin (K) [20].

This study uses the fluid's inlet velocity as the boundary condition. The relationship between the inlet flow rate and the inlet velocity is expressed as:

$$Q_2 = SV$$

In the formula: Q2 is the inlet flow rate of the fluid, in m³/s; S is the cross-sectional area of the inlet of the cooling pipe, in m²; V is the inlet velocity of the fluid, in m/s.

2.3. Mesh Generation for Fluids and Solids

The internal fluid domains of the inlet and outlet pipes, clamping head, and water cooling sleeve are extracted by volume extraction, followed by mesh generation. Figure 2 shows a sectional view of the mesh generation for the fluid domain and the simplified model of the burn-through device. The overall mesh generation method for the fluid domain is automatic, with a cell size of 5mm, while the cell size for other areas is 7mm. The mesh generation for the graphite electrode of the burn-through device uses a sweeping method, with a cell size set to 5mm. The clamping blocks, clamping head, inlet and outlet pipes, and water cooling sleeve use an automatic mesh generation method. The cell size for the clamping head and clamping blocks is set to 5mm, while the cell size for the remaining areas is set to 7mm.

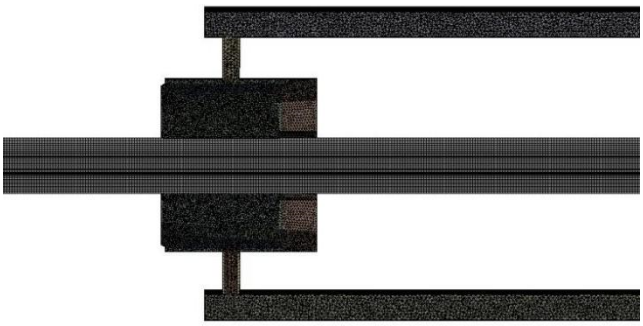

Fig 2. Grid division cross-section

2.4. Boundary Condition Setup

The cooling effect of the water is related to the fluid flow rate, which in turn depends on the fluid velocity. Several sets of different inlet fluid velocities are set, with the fluid inlet temperature set to 25°C. Due to the high temperature in the arc zone, which causes heat radiation to the surroundings, more than 30% of the arc energy can be transferred through radiation [15]. Therefore, a heat source is applied at the end face of the graphite electrode where the arc is generated. The resistivity of graphite decreases as the temperature increases, and it is set to decrease by 10%-20% at high temperatures. The burn-through device uses alternating current for the arc, and the temperature of the burn-through device is related to the current in the short network. The input current for the short network is alternating current, and the current magnitude is related to the contact between the conductive copper block and the electrode. This study uses steady-state calculations, with the short network current for the new discharge device set between 5000A and 10000A. The model input currents are set to 5000A and 10000A, with a calculation time of 1 second. The selected materials and specific parameters are shown in Table 1.

Table 1. Selected materials and some parameters

name	density/(kg·m^{-3})	thermal conductivity/(W·m^{-1}·K^{-1})		specific heat capacity/(J·kg^{-1}·K^{-1})
S31008	7980	100℃	16.3	500
		500℃	21.5	
316L	7980	100℃	15.1	502
		500℃	20.9	
liquid water	998.2	25℃	0.6	4182

According to the model, the input current passes through the graphite electrode and generates heat, which is directly transferred to the wedge block, affecting its temperature. Simultaneously, heat radiation is emitted to the surrounding environment, causing an increase in the ambient temperature. The outer surfaces of the wedge block and clamping head undergo convective heat transfer with the air, and the graphite electrode indirectly affects its temperature through thermal radiation.

3. TEMPERATURE SIMULATION ANALYSIS

3.1. Simulation Temperature Analysis of the Clamping Head

The heat in the clamping head comes from the graphite electrode. Firstly, the graphite electrode transfers heat to the wedge block through heat conduction, and the wedge block then transfers the

heat to the clamping head. Secondly, the graphite electrode radiates heat to the surrounding environment. When the input current is 5000A, and before water cooling is applied, the temperature field distribution for an inlet fluid velocity of 0.86 m/s is shown in Figures 3(a) and 3(b), respectively. In Figure 3(b), the lowest temperature is near the inlet of the water cooling system. The water temperature is low, and the flow velocity is at its maximum, which is why the temperature is lowest in this region.

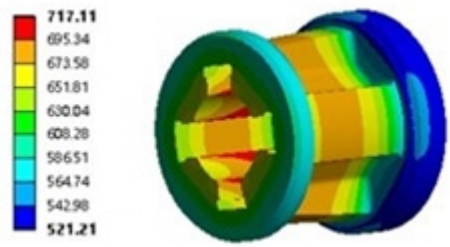

(a) Before water cooling is applied

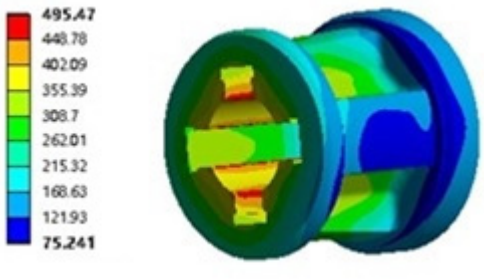

(b) After water cooling with an inlet velocity of 0.86 m/s

Fig 3. Temperature distribution of collet at 5000A

When the input current is 5000A, the curves of the minimum and maximum temperatures of the clamping head with respect to the change in fluid inlet velocity are shown in Figures 4(a) and 4(b), respectively. The temperature of the clamping head is below 800°C before water cooling is applied. After the liquid water cooling is introduced, both the maximum and minimum temperatures of the clamping head continuously decrease as the inlet flow velocity increases.

When the input current is 10000A, the temperature field distribution before water cooling and with an inlet fluid velocity of 0.86 m/s is shown in Figures 5(a) and 5(b), respectively. When the input current is 10000A, before water cooling, the temperature in the area where the clamping head contacts the wedge block exceeds 800°C, with a maximum temperature of 1061.7°C. After introducing liquid water cooling, with an inlet velocity of 0.86 m/s, the maximum temperature of the clamping head decreases to 797.58°C.

When the input current is 10000A, the curves of the minimum and maximum temperatures of the clamping head with respect to the change in fluid inlet velocity are shown in Figures 6(a) and 6(b), respectively. After reaching the critical value of the safe temperature, both the maximum and minimum temperatures of the clamping head continue to decrease as the inlet velocity of water in the water cooling system increases.

3.2. Simulation Temperature Analysis of the Wedge Block

When the input current is 5000A, the temperature field distribution of the wedge block before water cooling and with an inlet fluid velocity of 0.86 m/s is shown in Figures 7(a) and 7(b), respectively. Before water cooling is applied, the maximum temperature of the wedge block is 771.91°C, which is within the safe temperature range during the operation of the burn-through device.

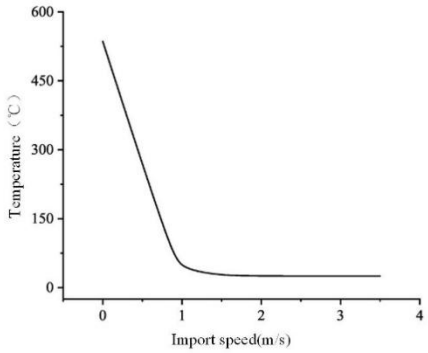

(a) The minimum temperature of the collet at 5000A

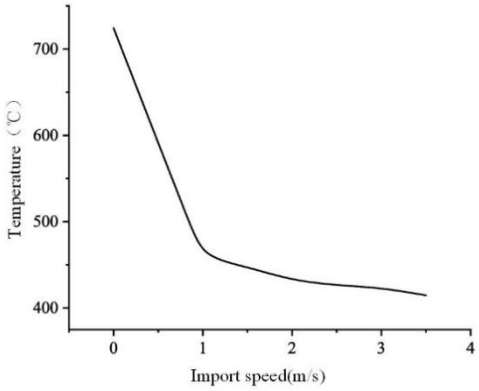

(b) The maximum temperature of the collet at 5000A

Fig 4. Temperature change curve of collet at 5000A

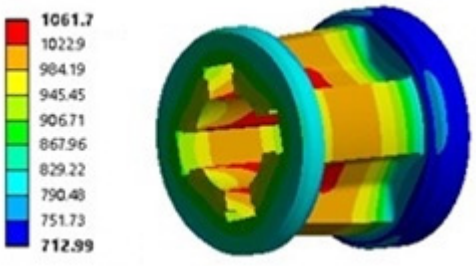

(a) Before water cooling is applied

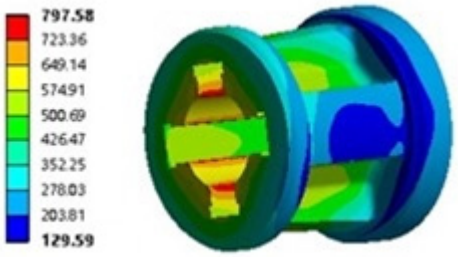

(b) After water cooling with an inlet velocity of 0.86 m/s

Fig 5. Temperature distribution of collet at 10000A

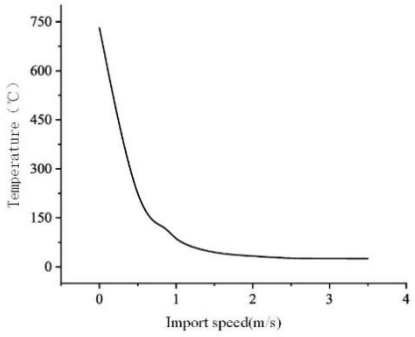

(a) The minimum temperature of the collet at 10000A

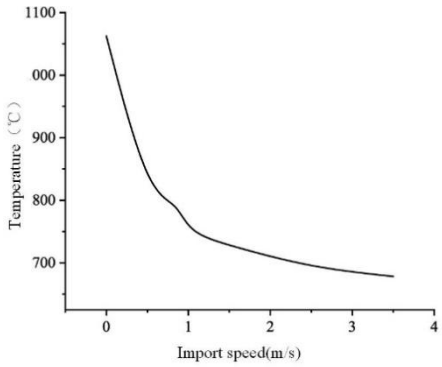

(b) The maximum temperature of the collet at 10000A

Fig 6. Temperature change curve of collet at 10000A

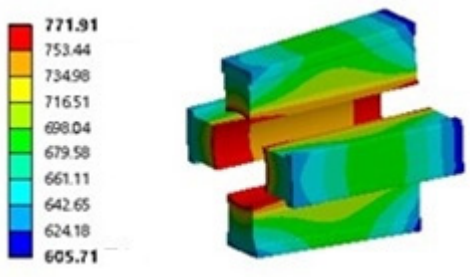

(a) Before water cooling is applied

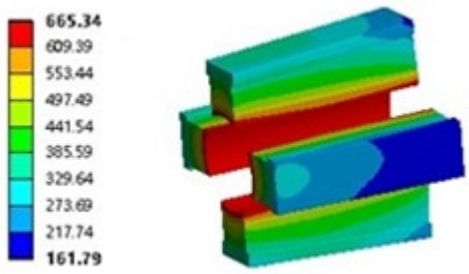

(b) After water cooling with an inlet velocity of 0.86 m/s

Fig 7. Temperature distribution of wedge clamping block at 5000A

When the input current is 5000A, the curves of the minimum and maximum temperatures of the clamping head with respect to the change in fluid inlet velocity are shown in Figures 8(a) and 8(b), respectively.

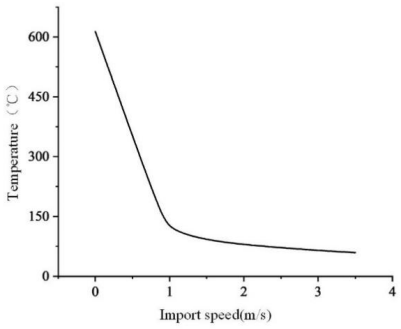

(a) The minimum temperature of the wedge clamping block at 5000A

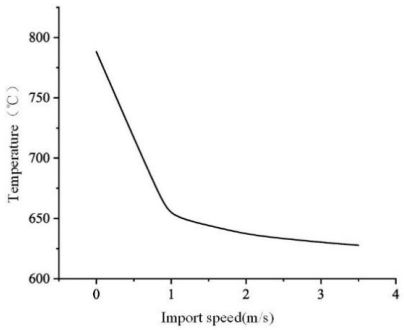

(b) The maximum temperature of the wedge clamping block at 5000A

Fig 8. Temperature variation curve of wedge clamping block at 5000A

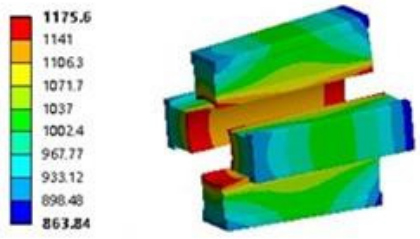

(a) Before water cooling is applied

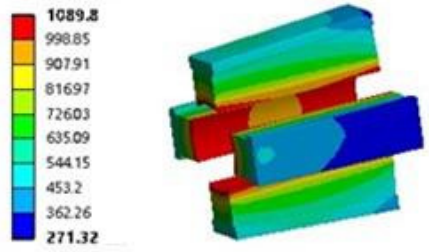

(b) After water cooling with an inlet velocity of 0.86 m/s

Fig 9. Temperature distribution of wedge clamping block at 10000A

When the input current is 10000A, the temperature field distribution of the wedge block before water cooling and with an inlet fluid velocity of 0.86 m/s is shown in Figures 9(a) and 9(b), respectively. Before water cooling is applied, the maximum temperature of the wedge block exceeds the material's continuous working temperature, and the entire wedge block's temperature is above the safe operating temperature of the burn-through device. After introducing liquid water cooling with an inlet velocity of 0.86 m/s, only the region close to the graphite electrode exceeds 800°C, while the temperature of the remaining areas stays below 800°C.

When the input current is 10000A, the curves of the minimum and maximum temperatures of the clamping head with respect to the change in fluid inlet velocity are shown in Figures 10(a) and 10(b), respectively. The maximum and minimum temperatures of the wedge block both continuously decrease as the inlet velocity increases.

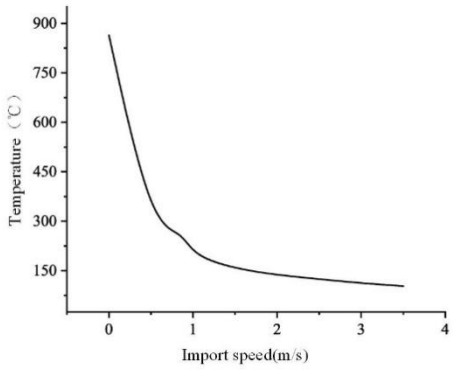

(a) The minimum temperature of the wedge clamping block at 10000A

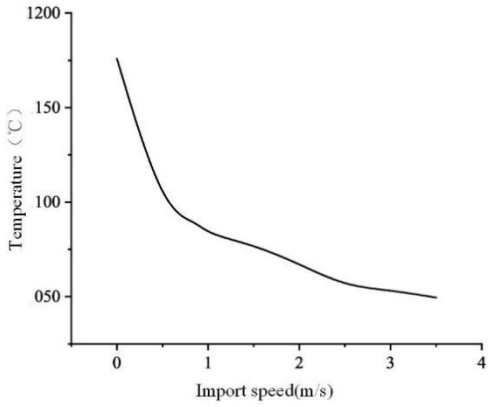

(b) The maximum temperature of the wedge clamping block at 10000A

Fig 10. Temperature variation curve of wedge clamping block at 10000A

4. CONCLUSION

This study simplifies the burn-through device model of the industrial silicon discharge robot designed by a certain company and analyzes the heating process of the burn-through device. Based on the principles of heat conduction, heat convection, and heat radiation, a coupled thermal-electric model of the graphite electrode and electrode clamping mechanism, along with the fluid temperature field, was established using ANSYS to simulate the temperature distribution during the operation of the burn-through device. The simulation results are as follows:

1. Before Water Cooling: When the current is 10000A, the maximum temperature of the clamping head exceeds 800°C, and the material's strength begins to decrease at temperatures above 800°C, which poses a safety risk for the operation of the burn-through device. The maximum temperature of the wedge block is 1175.9°C, which exceeds the material's continuous operating temperature.

2. After Water Cooling with 0.86 m/s Fluid Inlet Speed: The temperature of all areas of the clamping head is below 800°C, and the maximum temperature of the wedge block is also below the material's maximum continuous operating temperature. When the inlet flow rate of the water cooling system reaches a value that ensures the burn-through device operates within the safe working temperature, increasing the inlet velocity continuously lowers the temperature of both the clamping head and the wedge block. Therefore, the minimum inlet velocity of the water cooling system should not be less than 0.86 m/s. Based on equation$Q_2 = SV$, the flow rate is 42.54 L/min. This means that the minimum inlet flow rate for ensuring the safe and stable operation of the burn-through device with water cooling is 42.54 L/min.

ACKNOWLEDGMENTS

Funding Projects: Sichuan Provincial Science and Technology Program (2022SZYZF07); Panzhihua Advanced Manufacturing Technology Key Laboratory Open Fund (2022XJZD01); Process Equipment and Control Engineering Key Laboratory of Sichuan Provincial Universities Open Fund (GK202205); The University Students' Innovation and Entrepreneurship Training Program (cx2021068).

REFERENCES

[1] XI Fengshuo, XI Dongfei, CAI Hongzheng, et al. Enhanced removal of metal impurities from industrial silicon by metal-assisted chemical etching[J]. Chinese Journal of Nonferrous Metals,2022,32(10):3158-3168.

[2] YAN Baonian, DUAN Xijing. Design of large-capacity industrial silicon furnace[J]. Ferroalloys,2023,54(03):11-18.

[3] ZHAO Zhihao,Deng Jianmin. Application of intelligent discharge robot in closed calcium carbide furnace[J]. China Chlor-Alkali,2023,(09):37-40.

[4] Ma Zanyu. The application of the discharge robot in the discharge process[J]. China Salt Industry,2020(12):46-49.

[5] Xie Yan, Yu Ming, Guo Chenyang, et al. Development of a water-cooling device for electrical control system of packaging machine[J]. Shandong industrial technology,2018(15):66,2.

[6] Shanghai Liaoyuan Automation Technology Co. Forging press punch cooling device:CN202311028864.X[P]. 2023-09-19.

[7] B. Zhang, P. Jing, Z. Tie, et al. Design of external auxiliary water cooling equipment for transformer and simulation and experimental study of its heat dissipation characteristics[J]. Science and Industry,2023,23(8):247-254.

[8] Yue Xiaoyun. Simulation analysis of heat dissipation of water-cooled motor controller based on ANSYS[J]. Equipment Management and Maintenance,2023(9):29-30.

[9] Duan Hui-Qiang, Fu Bo, Jin Jide. An advanced IGBT thermal module design based on water cooling system[J]. Electronic Devices,2022,45(5):1082-1088.

[10] CHEN W, MAO Z, TIAN W. Water cooling structure design and temperature field analysis of permanent magnet synchronous motor for underwater unmanned vehicle[J]. Applied Thermal Engineering, 2024,240: 122243.

[11] Zhongye Dongfang Engineering Technology Co., Ltd. A Burn-through Device: CN201610815467.0[P]. 2017-01-11.

[12] Heihe Hesheng Silicon Industry Co., Ltd. An Industrial Silicon Burn-through Device: CN202321789584.6[P]. 2024-01-09.

[13] Ningxia Haisheng Industrial Co., Ltd. A High-Temperature Smelting Water-Cooled Burn-through Device: CN202122493325.6[P]. 2022-06-24.

[14] Liu Jianfeng. Simulation study on electrode control system of electric arc furnace for ferromanganese smelting[D]. Kunming University of Science and Technology,2011.

[15] JIANG Wenting, WEI Kuixian, LU Guoqiang, et al. Numerical simulation of arc initiation process in a mineral heat furnace for industrial silicon smelting[J]. Nonferrous Metal Engineering,2021,11(7):60-67,81.

[16] ZHANG Huazhen, HE Haibin, XIAO Jingjing, et al. Study on the temperature rise characteristics of relays under thermoelectric coupling[J]. Electromechanical Information, 2023, (08):9-11,16.

[17] WANG Wenlong, LIANG Huimin, ZHAI Guofu. Simulation analysis of electromechanical thermal coupling in contact system of sealed electromagnetic relay[J]. Electromechanical Components,2007(01):3-6,20.

[18] Ye Long. Design and simulation analysis of high-voltage DC relay electromagnetic system[D]. Xiamen Institute of Technology,2022.

[19] WANG Qi-Long, WANG Guo-Hai, CHEN Xiang-Rong, et al. Thermo-electric coupling simulation of 10 kV AC XLPE cable converted to DC operation[J]. Journal of Southwest Jiaotong University,2022,57(01):46-54.